ISSN 0016-7932, Geomagnetism and Aeronomy, 2022, Vol. 62, No. 3, pp. 288–304. © Pleiades Publishing, Ltd., 2022.

Study of Distribution and Asymmetry in Soft X-ray Flares over Solar Cycles 21–24

Amrita Prasad[a], *, Soumya Roy[b], Subhash Chandra Panja[a], and Sankar Narayan Patra[c], **

[a] *Department of Mechanical Engineering, Jadavpur University, Kolkata, West Bengal, 700032 India*

[b] *Department of Applied Electronics and Instrumentation Engineering, Haldia Institute of Technology, Haldia, Midnapore (E), West Bengal, 721657 India*

[c] *Department of Instrumentation & Electronics Engineering, Jadavpur University, Kolkata, West Bengal, 700106 India*

**e-mail: prasad.amrita1@gmail.com*

***e-mail: sankar.journal@gmail.com*

Received January 2, 2021; revised November 30, 2021; accepted January 27, 2022

Abstract—This paper investigates the North–South (N–S) as well as East–West (E–W) distribution and asymmetry in Soft X-ray flares (SXR) activity during the period 1976–2019 which corresponds to solar cycles 21–24. Our results reveal that, cycles 21, 22 and 23 are dominated by southern hemisphere and the cycle 24 is also found to be southern hemisphere dominated using soft X-ray flares data. The cumulative plot indicates a slight excess of X-ray flare events in the southern hemisphere during solar cycles 21, 23 and 24. A significant excess of flare events in the southern hemisphere has been observed in the cumulative plot during cycle 22. The most prolific latitude band in the N–S distribution is the 10°–20° which produced maximum number of soft X-ray flares over solar cycles 21, 22, 23 and 24 whereas no such longitudinal band is observed in the E–W distribution. The time-latitude plot of SXR flares is also constructed to study the behaviour of N–S distribution. It is also revealed in current work that the occurrence (number) of M and X class flares is showing a declining trend since solar cycle 21 till solar cycle 24 thereby violating the Gnevyshev-Ohl (G-O) rule. A significant eastern dominance is being observed till solar cycle 23 but the predominance shifted to western hemisphere during cycle 24. Our analysis reveals that the North–South asymmetry is highly significant in comparison to East–West asymmetry.

DOI: 10.1134/S0016793222030033

1. INTRODUCTION

Various solar activity features are observed to be non-uniformly distributed in relation to heliographic latitude (north–south) as well as longitude (west–east) across the solar disk (Joshi et al., 2010). This intrinsic feature of solar activity is termed as asymmetry. Many attributes of cyclic activity of the Sun are more clearly noticeable in the asymmetry of activity indicators rather than in the activity indicators themselves (Badalyan, 2012).

The N–S asymmetry in various indicators of solar activity provides evidence that the two hemispheres work differently and are governed by independent laws (Badalyan and Obridko, 2017) and the magnitude of the north-south asymmetry quantifies this difference (Badalyan, 2012). The North-South (N–S) distribution and asymmetry is being studied by many authors using different solar activity indices. Garcia (1990) study was based on the large X-ray flares from GOES satellite during solar cycle (SC) 20–21. The author reported that the large flares were initially more concentrated towards northern heliographic latitude but gradually started shifting towards southern part as the cycle progressed. The North-South asymmetry of SXR flare events of intensity class ≥M1 was studied by Li et al. (1998) throughout the maximum phase of 22nd cycle. They reported an overall southern hemisphere governance during that period. The latitudinal distribution as well as asymmetry of solar active prominence (SAP) events were studied by Verma (2000) over solar cycles (19-23). The author reported that SAP events were more concentrated in 11°–20° latitudinal band in both the hemispheres. Li et al. (2003) performed the study on north-south asymmetry of solar active prominence events at low (≤40°) as well as high (≥50°) latitudes in cycles (19-22). They observed that the asymmetry at low latitudes did not have any relation with the high latitudes. Using different limb and disk features of solar active prominence (SAP) and total SAP events, Li et al. (2003) found that SAP events were more concentrated in 21°–30° latitudinal band during cycle 23. Joshi et al. (2010) performed a statistical study on soft X-ray flares and observed a southern excess during solar cycle 21–23. The asym-

Table 1. The counts of different intensity classes, the total SXR flare counts and the corresponding percentage in brackets during SCs 21–24

Class	Number of SXR events in each solar cycle			
	SC 21	SC 22	SC 23	SC 24
B	2857 (14.38%)	6260 (29.95%)	8414 (36.39%)	5480 (39.77%)
C	14662 (73.78%)	12469 (59.65%)	13144 (56.84%)	7552 (54.81%)
M	2184 (10.99%)	2022 (9.67%)	1440 (6.23%)	702 (5.09%)
X	168 (0.85%)	153 (0.73%)	125 (0.54%)	45 (0.33%)
Total	19872 (100.00%)	20904 (100.00%)	23123 (100.00%)	13779 (100.00%)

metric behaviour of sunspot area, SAP events and Hα flares at low (≤40°), high (≥50°) and total latitudes was investigated by Bankoti et al. (2011). They reported a southern dominance during cycles 21–23 and northern dominance during cycle 20 at low-latitudes. Joshi et al. (2015) investigated the temporal evolution of soft X-ray flare (SXR) index over cycles 21, 22 and 23 and found that the asymmetry was significant during the evolutionary phases of solar cycles. Kramynin and Mikhalina (2018) analyzed the north-south asymmetry of latitude-longitude distribution of sunspot number from 1874–2013 and found that the north-south asymmetry of sunspot number exists for the latitude-longitude ranges where solar activity manifested.

In comparison to North-South asymmetry, the studies related to the east-west asymmetry in various indices of solar activity are very few. Letfus and Ruzickova-Topolova (1980) investigated the east-west asymmetry in Hα flare numbers spanning 1959–1976 and found a statistically significant E–W asymmetry only for specific time periods. Joshi (1995) using sunspot groups, filaments/Solar Active Prominence (SAP) and Hα flares data, observed a small eastern dominance in flare activity. Using X-ray flares events of class ≥M1, Li et al. (1998) did not observe any significant east-west asymmetry over the maximum period of 22nd solar cycle rather a non-uniform distribution of X-ray flare events was reported. Temmer et al. (2001) and Joshi and Pant (2005) reported a slight but significant eastern and western excess in Hα flares over cycles 21–22 and solar cycle 23 respectively. Verma (2000) did not observe any significant east-west asymmetry in SAP events during the period 1957–1998 which is in opposition with the study performed by Joshi et al. (2009) who observed a small E–W asymmetry in SAP data over cycle 23.

This paper investigates the North–South (N–S) as well as East–West (E–W) distribution and asymmetry of soft X-ray (SXR) flares events during the period 1976–2019 which corresponds to solar cycle 21, 22 and 23 and the almost complete solar cycle 24. The statistical significance of solar X-ray flare predominance in solar north and south as well as east and west hemisphere has been evaluated using binomial probability distribution method.

2. DATA

For the current work, we have used the soft X-ray flares (SXR) events for the time span of January, 1976 to May, 2019. The data has been downloaded from NOAA National Geophysical Data Center (NGDC): https://www.ngdc.noaa.gov/stp/space-weather/solar-data/solarfeatures/solar-flares/x-rays/goes/xrs/ and http://hec.helio-vo.eu/hec/hec_gui.php. A total of 77677 SXR events has been reported during the considered time period. For the purpose of analysis, the data has been grouped into four solar cycles which corresponds to solar cycle 21 (March 1976–September 1986), solar cycle 22 (September 1986–August 1996), solar cycle 23 (August 1996–December 2008) and solar cycle 24 (December 2008–May 2019). In the catalogue of SXR flare events, the heliographic information was not listed for some events. After eliminating those events, a total of 39892 SXR events for North-South and a total of 39776 SXR events for East–West, were used for distribution as well as asymmetry analysis.

Table 1 lists the total counts of SXR flare events as well as for the individual (B, C, M and X) classes reported during the considered time span irrespective of the heliographic information is being provided or not.

From Table 1 it can be observed that most of the flare activity in all the four solar cycles belongs to the C class. Also, the X class flare events contributed less in the flare activity during cycles 21–24. The C, M and X class flare activities in cycle 21 is more in comparison to solar cycles 22, 23 and 24. Figure 1 depicts the variations in monthly plot of total SXR counts and the counts of the individual intensity (B, C, M and X) classes.

3. METHOD

The normalized N–S and E–W asymmetry of the soft X-ray flare event counts are being defined by the asymmetry index which is being calculated using (Joshi et al., 2010)

$$AI = (N - S)/(N + S), \quad (1)$$

and

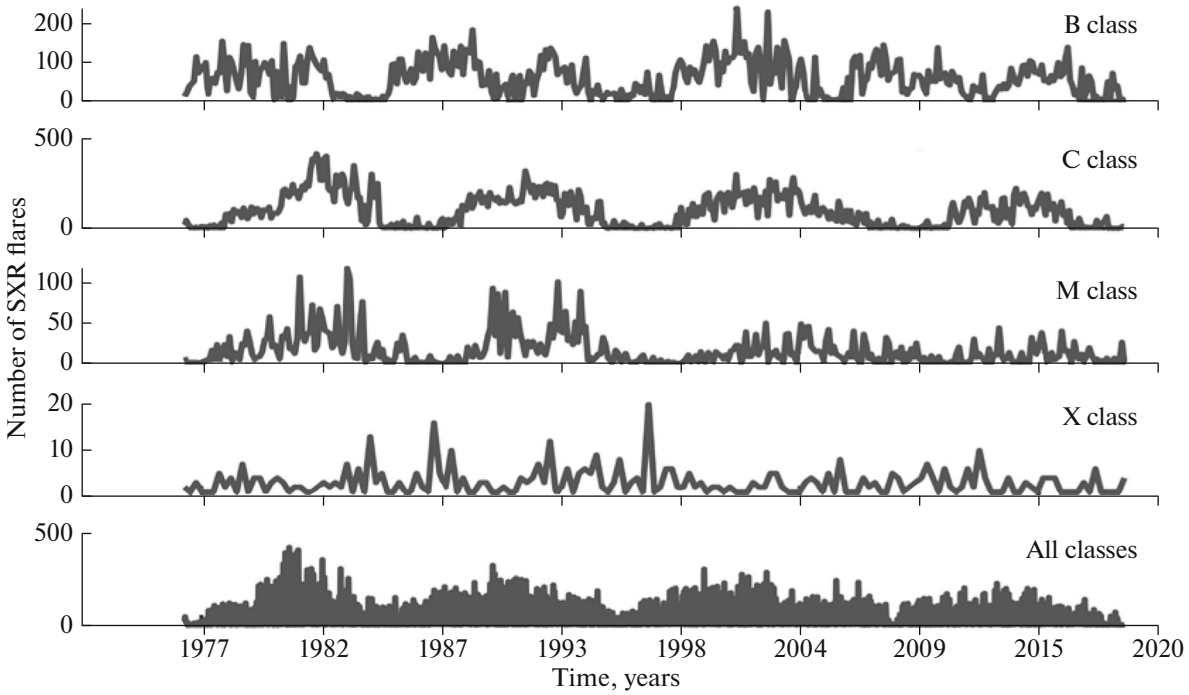

Fig. 1. Monthly plot of distinct intensity class counts as well as the total soft X-ray counts (B, C, M and X classes together) for the period 1976–2019.

$$A = (E - W)/(E + W). \quad (2)$$

The *AI* and *A* reflects the distribution of the solar X-ray flare activity in the north-south and east-west hemispheres respectively. S and N denote the occurrences of SXR flare events in solar south and north hemispheres. Similarly, W and E denote the occurrences of SXR flare events in the solar west and east hemispheres. If $AI > 0$, the solar X-ray flare activity is being governed by northern hemispheres and if $AI < 0$, southern hemisphere governs the solar X-ray flare activity. If $A > 0$, eastern hemisphere dominates the solar X-ray flare activity otherwise western hemisphere dominates the flare activity.

The statistical significance of solar X-ray flare predominance in solar north-south and east -west hemispheres has been evaluated by employing binomial probability distribution. The actual probability $P(m)$ of obtaining m objects in one class and $(n - m)$ objects in another (Li et al., 1998; Carbonell et al., 2007) is given by

$$P(m) = \frac{n!}{m!(n-m)!} p^m (1-p)^{(n-m)}, \quad (3)$$

where n corresponds to the number of objects in two classes. p corresponds to the occurrence probability of one flare event in a particular hemisphere, which is 0.5 or (1/2) for the current case. The probability to obtain more than d objects in one class is defined by (Vizoso and Ballester, 1990; Carbonell et al., 2007)

$$P(\geq d) = \sum_{m=d}^{n} P(m). \quad (4)$$

In general, $P(\geq d) > 10\%$ signifies a result which is statistically not significant (flare events in north and south hemisphere is considered to be equal); $5\% < P(\geq d) < 10\%$ signifies a result of marginal significance; $1\% < P(\geq d) < 5\%$ signifies a result of statistical significance (N–S asymmetry is an actual event and not because of random fluctuation) and $P(\geq d) < 1\%$ signifies a result which of high significance (Vizoso and Ballester, 1990).

3.1. N–S Distribution in Relation to Heliographic Latitude

For investigating the spatial distribution of soft X-ray flares events in relation to the heliographic latitudes, the soft X-ray flare events have been categorized into 6 latitudinal bands such as (0°–10°), (10°–20°), (20°–30°), (30°–40°), (40°–50°) and (>50°), for both solar north and south hemispheres during cycles 21–24 and is given in Tables 2–5.

From Tables 2–5, it can be observed that, maximum number of solar X-ray flare events occurred in the 10°–20° latitudinal band during all the considered solar cycles. Also, the dominant hemisphere is found to be southern hemisphere during solar cycles 21, 22, 23 and 24 having a highly significant probability value

Table 2. Yearly counts of SXR flare at various latitude bands in North and South hemispheres during SC 21. *AI* indicates the N–S asymmetry indices values, DH indicates the dominant hemisphere and dash (–) indicates that the probability values are insignificant

Years		Number of flares at different heliographic latitude						Total	*AI*	Probability	DH
		0°–10°	10°–20°	20°–30°	30°–40°	40°–50°	>50°				
1976	N	45	14	6	0	0	0	65	–0.1558	0.0317	S
	S	62	22	4	1	0	0	89			
1977	N	29	42	45	11	0	0	127	–0.0558	0.1967	–
	S	1	40	94	4	3	0	142			
1978	N	7	456	196	56	2	0	717	0.2568	1.78×10^{-18}	N
	S	5	199	191	27	1	1	424			
1979	N	220	489	163	43	1	0	916	0.2454	1.98×10^{-21}	N
	S	31	320	173	31	0	0	555			
1980	N	165	401	106	4	1	0	677	–0.0851	5.75×10^{-4}	S
	S	189	431	155	27	0	1	803			
1981	N	326	582	33	2	0	1	944	–0.0151	0.261	–
	S	340	511	102	4	16	0	973			
1982	N	362	548	50	0	0	0	960	0.0373	0.057	N
	S	321	483	87	0	0	0	891			
1983	N	72	149	30	0	0	0	251	–0.5882	6.58×10^{-10}	S
	S	364	519	80	5	0	0	968			
1984	N	135	184	15	0	0	0	334	–0.2400	5.52×10^{-13}	S
	S	194	348	3	0	0	0	545			
1985	N	137	6	0	0	0	0	143	–0.0435	0.244	–
	S	63	90	3	0	0	0	156			
1986	N	106	0	4	0	0	0	110	0.1518	0.021	N
	S	72	9	0	0	0	0	81			
Total	N	1604	2871	648	116	4	1	5244	–0.0352	1.11×10^{-4}	S
	S	1642	2972	892	99	20	2	5627			
Probability		0.258	0.095	1.61×10^{-10}	0.138	7.72×10^{-4}	0.375				
DH		–	S	S	–	S	–				

for solar cycle 21–23 and a statistically significant probability value for solar cycle 24.

Figure 2 depicts the histogram plot of latitudinal distribution of SXR flares between –50° to 50° latitudes during solar cycle 21–24. In the plot, 0° indicates the Sun's equator. For better understanding as to how the spatial asymmetry varies with distinct intensity classes (Joshi and Pant, 2005), the histograms are also separately plotted for B, C, M and X intensity classes. From Fig. 2 it can be observed that SXR flare events exhibit a marked histogram peak at 10°–20° latitudinal band for both positive (north) and negative(south) sides.

The magnetic dynamo in the Sun is believed to be the reason behind the Sun's magnetic field and is root to different solar manifestation. The solar dynamo model comprises of cyclic motion of two components (Parker, 1955; Pandey et al., 2015). The poloidal field component involves in the gas flow from equatorial to the polar region at the surface due to meridional circulation (Choudhuri, 2011) and in turn carries dynamo waves from polar to equatorial region from deep inside the Sun and hence plays a crucial role in magnetic dynamo of the Sun (Pandey et al., 2015). The toroidal field component generated at the solar convective zone base, manifests externally as sunspots and into flare activity which moves towards the equator (Pandey et al., 2015). The time-latitude plot of such activity give rise to butterfly diagram. For investigating the nature of distribution in case of SXR flares at different latitudes, the time-latitude plot of SXR flares has been constructed and depicted in Fig. 3 below.

It can be observed in Fig. 3 that the occurrence of high intensity class flares is rare near the 0°–5° lati-

Table 3. Yearly counts of SXR flare at various latitude bands in North and South hemispheres during SC 22. *AI* indicates the N–S asymmetry indices values, DH indicates the dominant hemisphere and dash (–) indicates that the probability values are insignificant

Years		Number of flares at different heliographic latitude						Total	*AI*	Probability	DH
		0°–10°	10°–20°	20°–30°	30°–40°	40°–50°	>50°				
1986	N	22	4	50	7	0	0	83	0.6436	1.86×10^{-11}	N
	S	7	3	7	1	0	0	18			
1987	N	10	35	78	39	1	0	163	–0.4340	2.62×10^{-26}	S
	S	9	19	267	117	1	0	413			
1988	N	4	289	306	69	0	0	668	–0.0585	0.0147	S
	S	6	298	373	69	5	0	751			
1989	N	39	398	365	103	3	0	908	–0.0243	0.1835	–
	S	35	539	323	53	0	0	950			
1990	N	138	566	194	76	1	0	975	0.0673	0.0022	N
	S	157	400	198	93	4	0	852			
1991	N	246	241	197	63	0	0	747	–0.3274	4.711×10^{-55}	S
	S	359	813	292	12	0	0	1476			
1992	N	226	334	47	0	0	0	607	–0.2178	4.42×10^{-18}	S
	S	320	496	123	6	0	0	945			
1993	N	313	279	9	0	0	0	601	0.1049	3.033×10^{-4}	N
	S	222	218	47	0	0	0	487			
1994	N	153	82	1	0	0	0	236	–0.0975	0.0143	S
	S	120	167	0	0	0	0	287			
1995	N	58	31	0	0	0	0	89	–0.4295	1.007×10^{-14}	S
	S	70	152	1	0	0	0	223			
1996	N	16	50	0	0	0	0	66	–0.1020	0.1241	–
	S	51	30	0	0	0	0	81			
Total	N	1225	2309	1247	357	5	0	5143	–0.1375	6.04×10^{-36}	S
	S	1356	3135	1631	351	10	0	6483			
Probability		0.005	1.98×10^{-29}	4.35×10^{-13}	0.423	0.151	–				
DH		S	S	S	–	–	–				

tude bands. However, the low intensity flares found to be majorly populating the ±5° latitude band.

The cumulative counts plots have also been plotted to represent the N–S distribution of flare events, initially introduced by Garcia (1990), is depicted in Fig. 4. The vertical separation between the black (solid line) and gray (dash-dotted line) provides the estimate of north/south excess till that time.

The north-south asymmetry indices of distinct intensity flare (B, C, M and X) classes and of total SXR flares have been calculated and is plotted in Fig. 5 below. Out of 43 estimated north-south asymmetry indices values, 28 values are highly significant, 4 values are observed to be statistically and 2 values to be marginally significant whereas 9 values are found to be insignificant. From Figure 5 it can be observed that the north-south asymmetry index values of distinct intensity flare classes and the total SXR flare approximately follows the same variations.

3.2. E–W Distribution with Respect to the Heliographic Longitudes

For investigating the spatial distribution of soft X-ray flares events in relation to heliographic longitudes, the SXR flare events has been categorized into 9 longitudinal bands such as (0°–10°), (10°–20°), (20°–30°), (30°–40°), (40°–50°), (50°–60°), (60°–70°), (70°–80°) and (80°–90°) for both East and West hemispheres during solar cycles 21–24 which is listed in Tables 6–9 below.

From Tables 6–9 it can be observed that there is no specific longitudinal band which is most prolific in producing SXR events during all the considered solar

Table 4. Yearly counts of SXR flare at various latitude bands in North and South hemisphere during SC 23. *AI* indicates the N–S asymmetry indices values, DH indicates the dominant hemisphere and dash (–) indicates that the probability values are insignificant

Years		Number of flares at different heliographic latitude						Total	*AI*	Probability	DH
		0°–10°	10°–20°	20°–30°	30°–40°	40°–50°	>50°				
1996	N	2	0	0	0	0	0	2	–0.9344	8.20×10^{-16}	S
	S	37	14	7	1	0	0	59			
1997	N	13	78	100	8	0	0	199	0.1775	6.49×10^{-4}	N
	S	2	48	79	10	0	0	139			
1998	N	3	234	171	19	1	0	428	–0.0573	0.0452	S
	S	0	138	326	13	3	0	480			
1999	N	46	388	274	31	4	0	743	0.0918	3.85×10^{-4}	N
	S	133	270	209	6	0	0	618			
2000	N	151	385	191	13	0	0	740	0.0207	0.2232	–
	S	82	464	147	17	0	0	710			
2001	N	165	378	100	0	0	0	643	–0.0795	0.0016	S
	S	171	445	117	19	2	0	754			
2002	N	108	337	96	2	0	0	543	–0.2044	2.17×10^{-14}	S
	S	257	451	111	3	0	0	822			
2003	N	195	153	12	0	0	0	360	–0.0438	0.1218	S
	S	120	220	46	6	0	1	393			
2004	N	347	433	7	4	10	19	820	–0.1603	7.42×10^{-13}	S
	S	418	695	2	6	5	7	1133			
2005	N	150	463	3	7	7	3	633	–0.2478	1.07×10^{-24}	S
	S	765	264	5	3	2	11	1050			
2006	N	38	30	0	0	2	1	71	–0.8289	1.49×10^{-146}	S
	S	513	242	0	2	1	1	759			
2007	N	39	2	0	0	0	0	41	–0.5543	9.80×10^{-15}	S
	S	132	10	0	0	1	0	143			
2008	N	1	0	0	4	0	0	5	–0.4118	0.0717	S
	S	8	4	0	0	0	0	12			
Total	N	1258	2881	954	88	24	23	5228	–0.1344	1.54×10^{-62}	S
	S	2638	3265	1049	86	14	20	7072			
Probability		8.59×10^{-95}	5.12×10^{-7}	0.0178	0.4698	0.072	0.3804				
DH		S	S	S	–	N	–				

cycles. From the corresponding probability values, it can be seen that the probability values are highly significant in case of solar cycle 21 and 22 and statistically significant for cycle 23 and 24. One interesting aspect observed in Tables 6–9 is that, the dominant hemisphere for solar cycles 21, 22 and 23 is found to be Eastern hemisphere while Western hemisphere dominates solar cycle 24.

Figure 6 below depicts the histogram plot of counts of total soft X-ray flare as well as of the distinct intensity (B, C, M and X) classes versus the heliographic longitudes during solar cycle 21–24. Western heliographic longitudes are being represented by negative sign (Li et al., 1998). From Figure 6 it can be seen that there is no marked peak in the histogram plots for total SXR flare events and for distinct intensity classes (B, C, M and X) during solar cycles 21–24.

Figure 7 depicts the cumulative count plot of soft X-ray flares in east (black solid line) and west (gray dashed line) hemispheres.

Figure 8 represents a plot between asymmetry index values and Time (years) for total SXR as well as different intensity class flares yearly counts during the period 1976–2019. Out of 43 east-west asymmetry indices value,

Table 5. Yearly counts of SXR flare at various latitude bands in North and South hemispheres during SC 24. *AI* indicates the N–S asymmetry indices values, DH indicates the dominant hemisphere and dash (–) indicates that the probability values are insignificant

Year		Number of flares at different heliographic latitude						Total	AI	Probability	DH
		0°–10°	10°–20°	20°–30°	30°–40°	40°–50°	>50°				
2009	N	0	9	5	2	0	0	16	0.2800	0.1148	–
	S	0	0	8	1	0	0	9			
2010	N	1	62	69	3	3	0	138	0.3463	3.97×10^{-7}	N
	S	0	16	49	2	0	0	67			
2011	N	50	331	84	0	0	1	466	0.2926	1.68×10^{-15}	N
	S	1	175	79	0	0	0	255			
2012	N	93	266	30	4	0	0	393	0.0051	0.4573	–
	S	7	279	103	0	0	0	389			
2013	N	128	162	28	0	0	0	318	–0.1642	3.33×10^{-6}	S
	S	101	282	59	1	0	0	443			
2014	N	127	152	1	0	0	0	280	–0.4292	1.36×10^{-42}	S
	S	148	485	68	0	0	0	701			
2015	N	142	210	9	0	0	0	361	–0.1624	1.05×10^{-6}	S
	S	98	338	65	0	0	0	501			
2016	N	119	107	3	0	0	0	229	0.4448	1.90×10^{-15}	N
	S	57	28	3	0	0	0	88			
2017	N	51	155	3	0	0	0	209	0.2783	5.81×10^{-7}	N
	S	91	27	0	0	0	0	118			
2018	N	17	14	0	0	0	0	31	–0.0462	0.4022	–
	S	29	5	0	0	0	0	34			
2019	N	53	2	0	0	0	0	55	1	–	–
	S	0	0	0	0	0	0	0			
Total	N	781	1470	232	9	3	1	2490	–0.0209	0.0689	S
	S	532	1635	434	4	0	0	2605			
Probability		3.34×10^{-12}	0.0016	2.10×10^{-16}	0.1333	–	–				
DH		S	S	S	–	–	–				

20 values are found to be highly significant, 4 values are statistically significant while 4 values are marginally significant and 15 values are found to be insignificant.

4. DISCUSSION

In the current work, the data of SXR flare events have been analyzed for solar cycles 21, 22, 23 and an almost complete solar cycle 24 (period covering from 1976–2019). Table 1 lists the total soft X-ray flare event counts as well as the counts of distinct intensity (B, C, M and X) classes during solar cycle 21–24. From Table 1 it is observed that most of flare activity during solar cycles 21–24 belongs to the C class while the X class flare events contributed less in the flare activity. The occurrence (number) of M and X class flares is continuously decreasing from solar cycle 21 to solar cycle 24 thereby disobeying the Gnevyshev-Ohl (G-O) rule which states that the an odd-number cycle should be stronger than the even-numbered cycle (Gnevyshev and Ohl, 1948). In the present context, cycle pair (22, 23) found to be violating the G-O rule. Komitov and Bonev (2001) investigated the condition for Gnevyshev-Ohl (G-O) rule violation which occurs when the even-numbered cycle is stronger than the odd-numbered cycle. Violation of Gnevyshev-Ohl rule for cycle pair (22, 23) has also been reported by Joshi et al. (2006) using Hα flare data and by Javaraiah (2016) using small and large sunspots group activity. From Table 1 it is also being observed that the number of low intensity flare (B class flares) are less during a strong solar cycle, in comparison to weak solar cycle. Also, solar cycle 24 is observed to be the weakest in

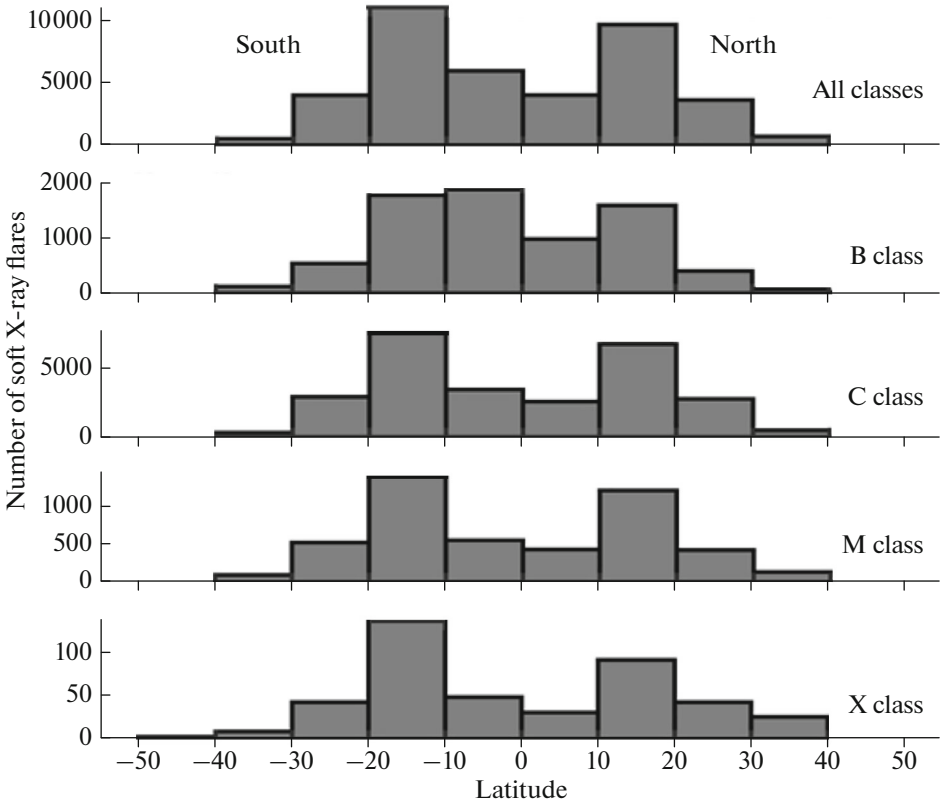

Fig. 2. Histogram plot of B, C, M and X intensity classes and the total soft X-ray counts (all classes together) versus the heliographic latitudes during solar cycles 21–24.

terms of flaring activity (a total of 13779 counts of flares) as compared to previous cycles.

In Figure 1, the occurrence of B class flare events is more observable during the minimum of solar cycles as compared to solar cycles maximum where flares of other intensity classes dominate. It is mainly because the X-ray background emission is found to be intense due to many solar events at the time of solar maximum, and hence the low intensity flares are difficult to detect during full-disk measurements (Feldman et al., 1997; Joshi et al., 2010).

Tables 2–5 depict the evolutionary aspect of soft X-ray flares during solar cycles 21, 22, 23 and 24. It is very interesting to observe that during the onset of solar cycles 21 and 23, 0°–10° latitude band is more active in producing flares and is generally southern hemisphere dominated with a statistically and highly significant probability values. But for solar cycles 22 and 24, 20°–30° latitude band more actively produced flares at the beginning and is observed to be northern hemisphere dominated although the corresponding probability value is highly significant for solar cycle 22 and is insignificant for cycle 24. The dominant hemisphere during the solar cycle minimum is generally the remnant of the previous cycle. In 1977, 1987, 1997 and 2009, just after the solar minimum, 20°–30° latitude band produced majority of the flares. With the progression of solar cycle, the solar X-ray flares occurrences show a drift to lower latitudes. Also, after the solar maximum, latitude ≥40° plays negligible role and the lower latitude bands 0°–10° and 10°–20° mostly supports the solar activity till solar minimum during cycles 21, 22, 23 and 24. This is because of larger zonal and meridional flow which contributes in producing a large number of flares at middle as well as at low latitudes (Pandey et al., 2015). The 10°–20° latitudinal band overall produced maximum number of soft X-ray flares events with a total of 5842, 5442, 6145 and 3109 SXR flares counts during solar cycle 21, 22, 23 and 24 respectively and is found to be dominated by southern hemisphere. In Figure 2, a marked peak at 10°–20° latitudinal band in both the hemispheres during solar cycles 21–24 for total SXR flares events as well as the SXR flares of individual intensity classes is being observed which further validates the obtained result. Verma (2000) found that SAP events were more concentrated in 11°–20° latitudinal band in both the hemispheres during solar cycles (19–23). Joshi et al. (2006) using Hα flare data during solar cycle 23 reported similar observations. Our obtained result is in accordance with the above studies using soft X-ray flare data. However, in Fig. 6 no significant peak is being observed in any longitudinal bands in E–W distribution of SXR flares.

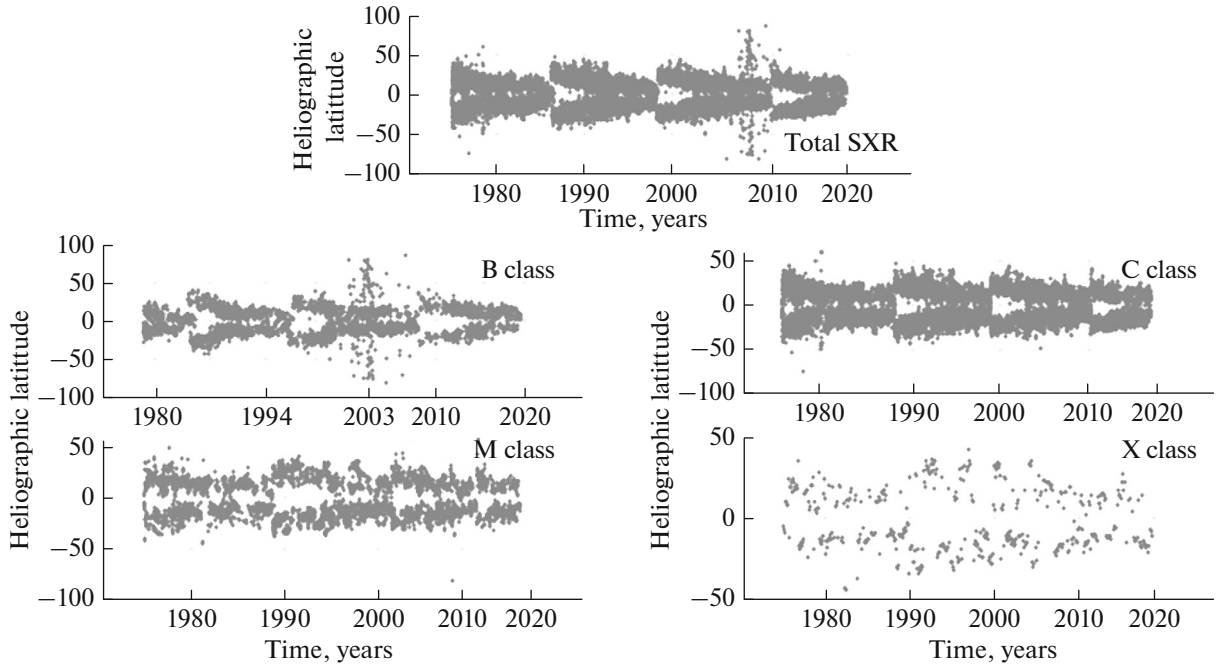

Fig. 3. Plots of latitudinal distribution of different intensity (B, C, M and X) classes as well as the total soft X-ray flares (all classes together) versus Time (years) during solar cycles 21–24.

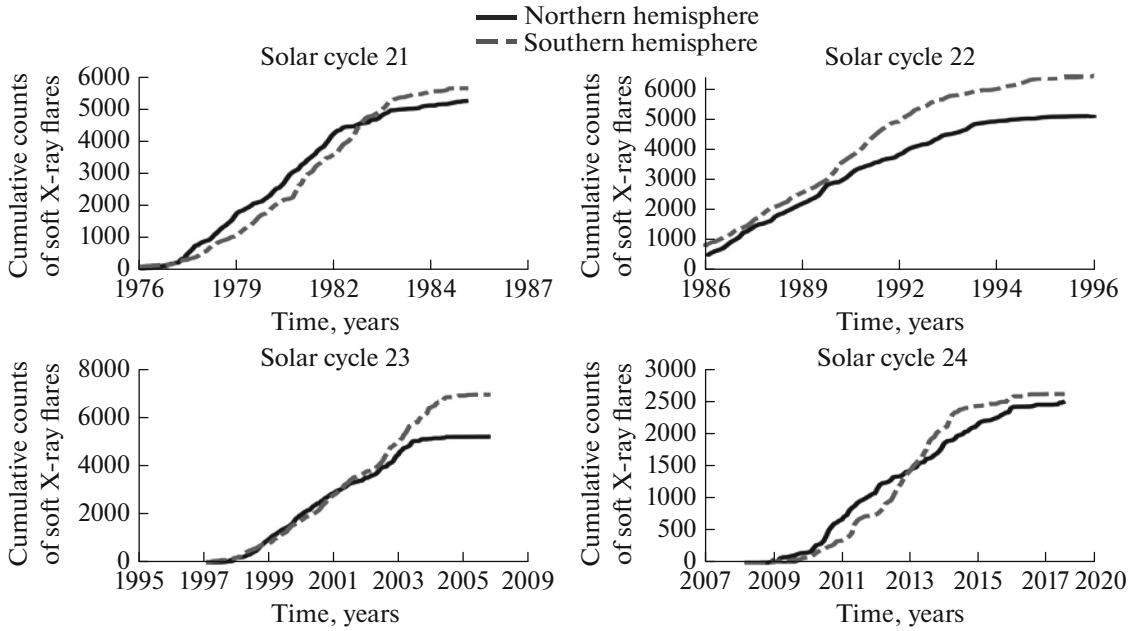

Fig. 4. Cumulative counts plot of soft X-ray flares events in the solar north (black solid line) and south (gray dash-dotted line) hemispheres during the period 1976–2019 (solar cycles 21–24).

In this paper we have tried to construct the time-latitude plot using the solar X-ray flares data to study the distributional behaviour of different intensity classes. From Figure 3 it can be observed that the high intensity class flares are rare near the 0°–5° latitude bands. Also, from Fig. 3 it can be seen that the flares do occur near ±5° latitude band (near equatorial region). The flares that are occurring near the ±5° latitude band are of low intensity and observed to be majorly contributing in the overall flaring activity.

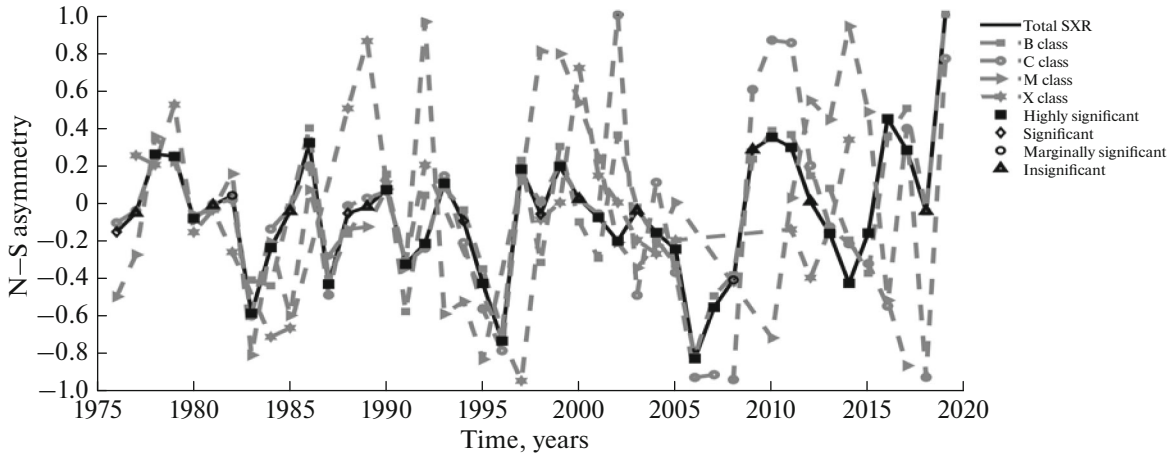

Fig. 5. N–S Asymmetry index values vs. Time (years) plots of distinct intensity (B, C, M and X) classes and total SXR flares during the period 1976–2019 (solar cycles 21–24).

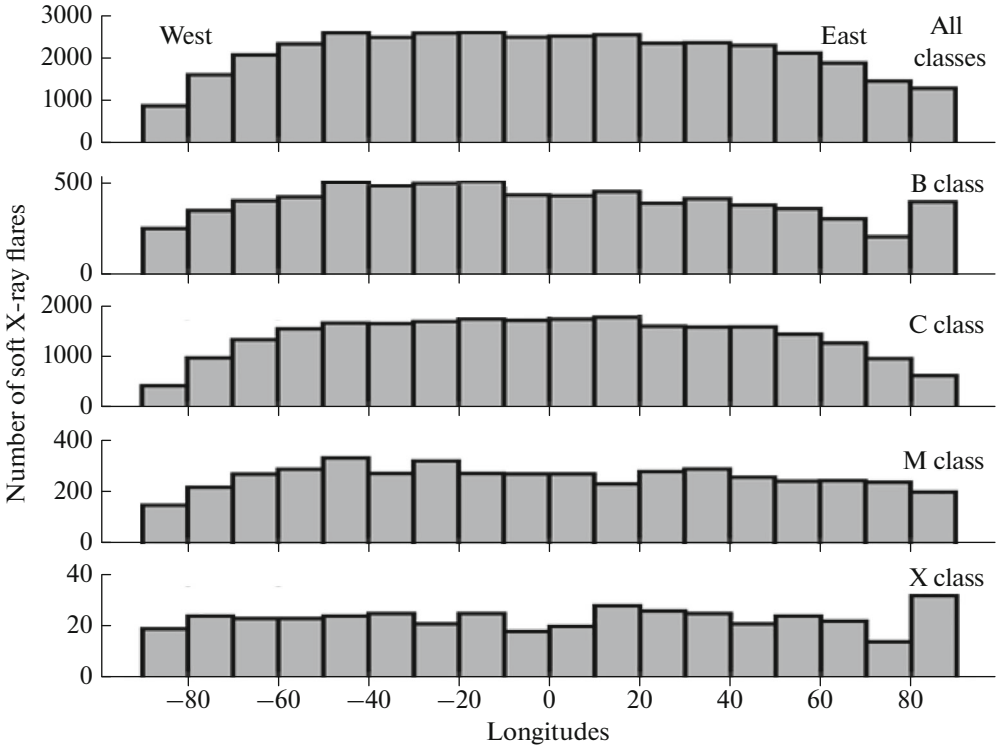

Fig. 6. Histogram plots of distinct intensity (B, C, M and X) classes and of the total soft X-ray flares counts (all classes together) versus the heliographic longitudes during solar cycles 21–24.

However, the solar X-ray flares events are observed to be spread in all longitudes.

Figure 4 gives a clearer picture of when the hemispheric dominance altered during solar cycles 21, 22, 23 and 24. During cycle 21, initially an excess of flares occurred in north hemisphere. But about 4 years before the end of the cycle the northern excess falls off and a very small south excess prevails till the end of the cycle (51.76% south, 48.24% north). A similar behaviour was reported by Viktorinová and Antalová (1991) using LDE X-ray flares and by Temmer et al. (2001) using Hα flares. For cycle 22, a small southern excess in X-ray flare counts is observed till 1989 (ascending and maximum phase) which is significantly enhanced after the maximum phase (44.24% North, 55.76% South). Temmer et al. (2001) observed

Table 6. Yearly counts of SXR flare events in 9 longitude bands in East and West hemispheres during solar cycle 21. *A* indicates the E–W asymmetry indices values, DH indicates the dominant hemisphere and dash (–) indicates that the probability values are insignificant

Year		Heliographic longitude									Total	*A*	Probability	DH
		0°–10°	10–20°	20°–30°	30°–40°	40°–50°	50°–60°	60°–70°	70°–80°	80°–90°				
1976	E	9	9	12	10	17	11	9	13	1	91	0.1818	0.0146	E
	W	7	10	7	11	11	5	4	2	6	63			
1977	E	19	14	17	15	27	23	11	18	10	154	0.1493	0.0085	E
	W	21	18	20	7	8	16	13	10	1	114			
1978	E	63	75	66	58	70	77	78	33	22	542	–0.0474	0.0581	W
	W	55	76	85	68	70	66	77	53	46	596			
1979	E	93	98	111	104	84	87	73	60	33	743	0.0178	0.2565	–
	W	117	103	87	86	83	83	79	54	25	717			
1980	E	111	95	107	89	119	92	86	63	20	782	0.0639	0.0076	E
	W	110	101	90	77	81	82	65	56	26	688			
1981	E	118	111	124	150	123	99	77	76	27	905	–0.0478	0.0195	W
	W	139	145	137	159	144	86	82	59	45	996			
1982	E	127	136	158	110	113	113	79	62	31	929	0.0119	0.3120	–
	W	154	152	130	107	111	93	77	55	28	907			
1983	E	77	89	76	88	100	94	75	49	23	671	0.1082	9.24×10^{-5}	E
	W	81	70	59	89	65	70	55	35	16	540			
1984	E	57	60	56	62	81	65	48	27	23	479	0.1011	0.0016	E
	W	55	55	52	55	43	46	46	31	8	391			
1985	E	29	30	21	12	16	24	19	7	14	172	0.1701	0.0021	E
	W	11	12	24	19	6	20	15	11	4	122			
1986	E	24	18	13	12	20	14	20	10	3	134	–0.0791	0.0985	W
	W	23	31	17	16	21	14	17	9	9	157			
Total	E	727	735	761	710	770	699	575	418	207	5602	–0.0790	0.0015	E
	W	773	773	708	694	643	581	530	375	214	5291			
Probability		0.1226	0.1703	0.0874	0.3445	3.98×10^{-4}	5.33×10^{-4}	0.0928	0.0679	0.3850				
DH		–	–	E	–	E	E	E	E	–				

similar tendency during solar cycle 22 using Hα flares. For solar cycle 23, till 1996 (minimum phase) a slight southern excess is seen. However, during 1997–2001 (ascending and maximum phase) a slight northern excess is observed and then southern excess of flares is observed after the solar maximum till the end of the solar cycle (57.49% south, 42.50% north). Similar behaviour was observed by Li et al. (2003) and Chowdhury (2013) using sunspot activities. During solar cycle 24, a slight northern excess in flare is seen till first maximum (2012) but after that a very slight southern excess is seen till 2019 (51.13% south, 48.87% north). Hence, using soft X-ray flares data, we found that the southern hemisphere predominates during solar cycles 21, 22 and 23. Our results also reveal that the solar cycle 24 is southern hemisphere dominated identical to cycles 21, 22 and 23 and validates the inference drawn by Verma (2000) and Li et al. (2009, 2009a).

From Figures 5 and 8 it can be seen that the north-south asymmetry is highly significant in comparison to East-West asymmetry.

The N–S asymmetry is now generally accepted as an actual phenomenon and many authors during the years have tried to give reasonable explanations behind the observed north-south asymmetry in various solar activity indicators. Bai (1987, 1988) proposed the concept of *superactive regions*. These are large and complex active regions comprising of sunspots giving rise to majority of solar flares and is frequently visible in certain regions of the Sun, called the active zones that possibly exists for more than one solar rotation. Hence the N–S asymmetry is may be due to the presence of the active zones in solar north and south hemispheres of the Sun, that can stay over for longer period of time (Temmer et al., 2001). The Babcock-Leighton process

Table 7. Yearly counts of SXR flare events in 9 longitude bands in East and West hemispheres during solar cycle 22. *A* indicates the E–W asymmetry indices values, DH indicates the dominant hemisphere and dash (–) indicates that the probability values are insignificant

Year		Heliographic longitude									Total	*A*	Probability	DH
		0°–10°	10°–20°	20°–30°	30°–40°	40°–50°	50°–60°	60°–70°	70°–80°	80°–90°				
1986	E	12	9	3	5	12	4	5	22	0	72	0.1077	0.1271	–
	W	6	10	7	9	8	4	3	10	1	58			
1987	E	30	41	29	36	33	33	38	25	22	287	0.0053	0.4667	–
	W	43	39	42	41	39	26	31	13	10	284			
1988	E	105	79	112	101	88	88	88	52	41	754	0.0718	0.0038	E
	W	92	109	74	82	76	78	62	50	30	653			
1989	E	135	115	131	109	113	129	111	90	63	996	0.0779	4.37×10^{-4}	E
	W	130	113	112	118	85	92	76	74	52	852			
1990	E	112	135	150	137	123	126	84	82	26	975	0.0732	9.74×10^{-4}	E
	W	120	112	102	92	111	98	88	82	37	842			
1991	E	133	148	131	134	152	130	131	80	44	1083	–0.0168	0.2215	–
	W	143	118	161	144	156	132	122	83	61	1120			
1992	E	96	86	90	114	114	75	72	50	26	723	–0.0629	0.0073	W
	W	98	123	110	119	95	120	75	50	30	820			
1993	E	64	83	77	67	78	77	56	49	16	567	–0.0307	0.0411	W
	W	90	85	65	59	71	50	47	27	15	509			
1994	E	32	47	35	30	26	21	30	23	9	253	0.0539	0.2558	–
	W	33	27	38	36	46	32	36	18	3	269			
1995	E	24	25	21	22	28	19	15	5	5	164	0.0547	0.1821	–
	W	25	23	25	20	15	15	10	9	5	147			
1996	E	2	11	6	3	8	3	4	2	2	41	–0.4058	1.04×10^{-6}	W
	W	12	13	11	12	11	12	13	9	4	97			
Total	E	745	779	785	758	775	705	634	480	254	5915	0.2283	0.0072	E
	W	792	772	747	732	713	659	563	425	248	5651			
Probability		0.1203	0.4395	0.1723	0.2586	0.0569	0.1115	0.0215	0.0363	0.4117				
DH		–	–	–	–	E	–	E	E	–				

of poloidal field generation is thought to be reason behind the observed irregularity in solar cycles (Goel and Choudhuri, 2009). Hemispherical asymmetry is also being explained in terms of difference in the amplitude of the meridional circulation in north and south hemispheres (Belucz and Dikpati, 2013) that continues for more than one solar cycle (Shetye et al., 2015). Schüssler and Cameron (2018) revealed that the hemispherical asymmetry can also be explained by superposition of two dynamo modes a dipolar modes of 22 years magnetic periods and a quadrupolar mode with periods between 12–15 years. All the above mechanisms are the possible interpretation to understand how the two hemispheres works and the possible cause of N–S asymmetry. However, no strong physical explanations have been found till date and the N–S asymmetry is still puzzling.

In case of E–W asymmetry analysis, an eastern dominance is being observed having highly and statistically significant probability values during solar cycle 21, 22 and 23 from Tables 6–9. However, a western predominance with a statistically significant probability values is being observed during solar cycle 24. Also, most of the longitudinal bands whose probability values are marginally, statistically or highly significant during cycles 21, 22 and 23 is found to be eastern hemisphere dominated while during solar cycle 24, longitudinal bands are observed to be mostly western hemisphere dominated.

Table 8. Yearly counts of SXR flare events in 9 longitude bands in East and West hemispheres during solar cycle 23. *A* indicates the E–W asymmetry indices values, DH indicates the dominant hemisphere and dash (–) indicates that the probability values are insignificant

Year		Heliographic longitude									Total	*A*	Probability	DH
		0°–10°	10°–20°	20°–30°	30°–40°	40°–50°	50°–60°	60°–70°	70°–80°	80°–90°				
1996	E	1	5	4	2	6	0	3	0	0	21	–0.4247	1.86×10^{-4}	W
	W	8	3	3	6	3	3	3	20	3	52			
1997	E	28	33	25	15	21	19	19	14	5	179	0.0529	0.1783	–
	W	28	31	19	18	17	19	10	11	8	161			
1998	E	66	48	54	58	50	58	41	25	8	408	–0.1013	0.0013	W
	W	61	80	61	63	61	66	48	36	24	500			
1999	E	88	97	96	81	83	90	70	38	20	663	0.0685	0.0085	E
	W	72	85	68	66	81	58	74	49	25	578			
2000	E	92	90	87	80	108	88	93	60	18	716	–0.0028	0.4685	W
	W	94	80	73	96	105	99	82	64	27	720			
2001	E	125	112	108	99	76	67	54	46	15	702	0.0123	0.3337	–
	W	99	102	97	72	89	79	65	55	27	685			
2002	E	107	87	104	97	89	58	68	40	9	659	–0.0186	0.2563	–
	W	83	95	81	95	89	73	78	61	29	684			
2003	E	42	48	50	32	33	35	37	28	139	444	0.0079	0.4199	–
	W	51	46	57	61	65	71	44	28	14	437			
2004	E	115	109	95	124	122	115	102	84	138	1004	0.0351	0.0641	E
	W	101	101	83	71	85	68	79	91	257	936			
2005	E	94	140	96	92	114	80	94	109	40	859	0.0908	1.72×10^{-4}	E
	W	78	53	53	60	60	75	64	64	209	716			
2006	E	30	31	31	46	41	33	57	103	3	375	–0.0518	0.0775	W
	W	68	53	55	46	35	31	24	26	78	416			
2007	E	8	3	14	20	30	19	16	15	2	127	0.3804	1.32×10^{-7}	E
	W	5	12	6	8	5	4	6	6	5	57			
2008	E	2	1	6	1	1	1	1	2	7	22	0.375	0.0251	E
	W	1	1	2	2	2	1	0	0	1	10			
Total	E	798	804	770	747	774	663	655	564	404	6179	0.0187	0.0201	E
	W	749	742	658	664	697	647	577	511	707	5952			
Probability		0.1112	0.0604	0.0016	0.0145	0.0237	0.6807	0.0141	0.0564	3.85×10^{-20}				
DH		–	E	E	E	E	–	E	E	W				

Table 9. Yearly counts of SXR flare events in 9 longitude bands in East and West hemispheres during solar cycle 24. *A* indicates the E–W asymmetry indices values, DH indicates the dominant hemisphere and dash (–) indicates that the probability values are insignificant

Year		Heliographic longitude									Total	*A*	Probability	DH
		0°–10°	10°–20°	20°–30°	30°–40°	40°–50°	50°–60°	60°–70°	70°–80°	80°–90°				
2008	E	0	0	0	0	0	0	0	0	0	0	0	0	–
	W	0	0	0	0	0	0	0	0	0	0			
2009	E	3	13	12	2	5	13	1	4	10	63	0.8261	2.24×10^{-13}	E
	W	1	3	1	0	0	1	0	0	0	6			
2010	E	16	37	41	18	10	36	15	39	7	219	0.3905	1.67×10^{-12}	E
	W	21	21	13	11	6	6	8	5	5	96			
2011	E	49	51	51	52	64	35	41	22	13	378	0.0356	0.1774	E
	W	41	39	40	54	55	42	45	31	5	352			
2012	E	49	76	60	53	41	46	39	15	18	397	–0.0364	0.1562	W
	W	59	69	61	44	50	41	49	35	19	427			
2013	E	52	46	64	55	49	52	29	27	2	376	0.0080	0.4274	–
	W	46	76	48	51	30	56	29	21	13	370			
2014	E	58	63	40	64	67	39	35	36	4	406	–0.1497	2.08×10^{-6}	W
	W	58	58	74	78	80	67	67	55	12	549			
2015	E	56	27	28	45	42	24	58	12	1	293	–0.2259	2.74×10^{-10}	W
	W	55	58	64	65	69	55	41	48	9	464			
2016	E	19	6	17	28	26	19	16	24	6	161	0.0915	0.0650	E
	W	18	15	18	14	14	29	14	9	3	134			
2017	E	13	3	4	14	9	4	24	2	1	74	–0.4498	4.84×10^{-14}	W
	W	5	20	21	27	42	28	26	16	10	195			
2018	E	3	1	3	1	7	6	7	2	46	76	0.2258	0.0075	E
	W	1	13	10	6	4	6	4	4	0	48			
2019	E	1	10	7	6	11	5	4	10	25	79	0.5490	1.14×10^{-8}	E
	W	0	1	2	0	12	4	3	1	0	23			
Total	E	319	333	327	338	331	279	269	193	133	2522	–0.0274	0.0251	W
	W	305	373	352	350	362	335	286	225	76	2664			
Probability		0.3014	0.0711	0.1785	0.3375	0.1272	0.0132	0.2485	0.0647	4.89×10^{-5}				
DH		–	W	–	–	–	W	–	W	E				

From the cumulative plots in Fig. 7, it can be observed that a slight but continuous eastern excess is observed during solar cycles 21, 22 and 23, (51.43% East, 48.57% West), (51.14% East, 48.86% West) and (50.94% East, 49.06% West) respectively. However, a slight western excess is observed during solar cycle 24 (48% East, 51.36% West). Temmer et al. (2001) reported a small but significant E–W asymmetry with a prolonged Eastern excess in Hα flares during solar cycles 21 and 22. Joshi (1995) also observed a small Eastern dominance for flare activity during solar cycle 22. However, Li et al. (1998) using X-ray flares events of intensity class ≥M1 did not observe any significant E–W asymmetry but reported a non-uniform distribution of X-ray flare events in longitudes over the maximum phase of cycle 22. Joshi and Pant (2005) reported a slight but significant western excess during solar cycle 23 using Hα flares. Our result of Eastern predomi-

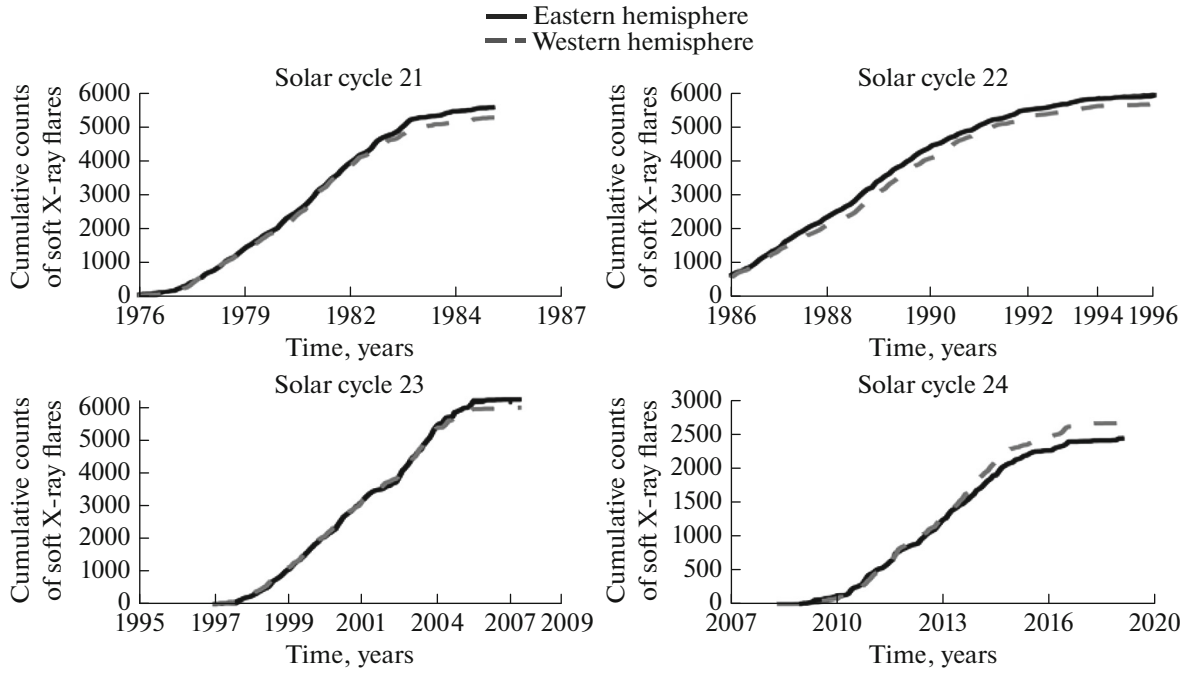

Fig. 7. Cumulative counts plot of monthly soft X-ray flares events in the solar east (black solid line) and west (gray dashed line) hemispheres during the period 1976–2019 (solar cycles 21–24).

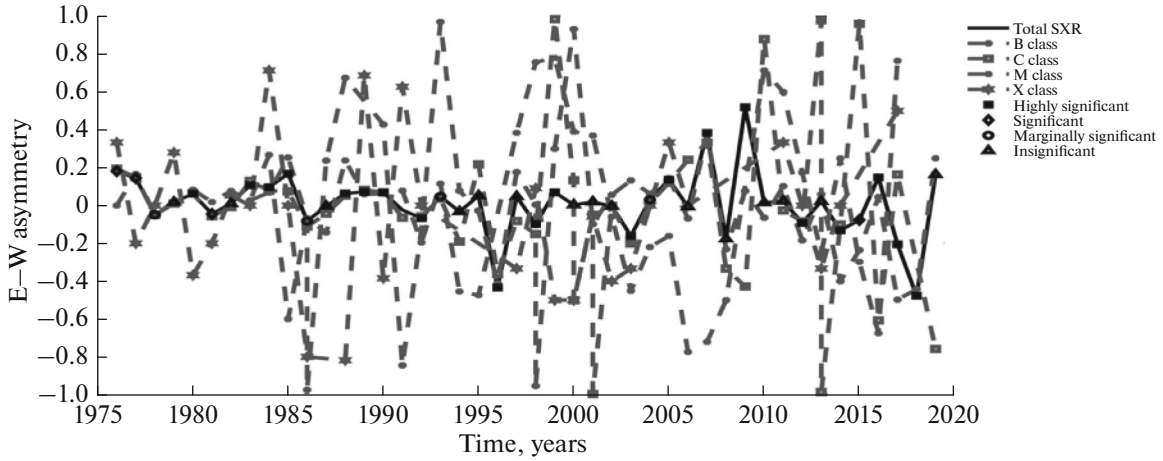

Fig. 8. E–W Asymmetry index values vs. Time (years) plots for total soft X-ray flares as well as for the distinct intensity classes during the period 1976–2019 (solar cycles 21–24).

nance during solar cycle 23 using SXR flares is in variance with Joshi and Pant (2005). Heras et al. (1990) found that the flares showed non-uniform distribution across longitudes and cannot be accounted for the observed E–W asymmetry but might be due to the transit of active zones on the solar disc. However, Heras et al. (1990) also observed a pronounced and prolonged E–W asymmetry in Hα flare data during the period of 1976–1985. A number of studies on E–W asymmetries using different solar activity indicators have been done but no possible explanation has been worked out till date and it remains a controversial issue. However, it is interesting to observe that the behaviour of E–W asymmetry has been altered during solar cycle 24 and the cycle 24 shows a predominance of Western hemisphere.

5. CONCLUSIONS

The present work has leads to following conclusions:

(a) The counts of C, M and X class flares are found to less in cycle 24 in comparison to cycles 21, 22 and 23 indicating the solar cycle 24 to be a weak cycle.

(b) The occurrence (number) of M and X class flares is continuously decreasing from solar cycle 21 to solar cycle 24 thereby disobeying the Gnevyshev-Ohl (G-O) rule for the solar cycle pair (22, 23).

(c) The 10°–20° latitudinal band produced maximum number of soft X-ray flares during solar cycles 21 to 24 in the study of the N–S distribution and is found to be dominated by southern hemisphere.

(d) After the solar maximum the higher latitude ≥40° plays negligible role in flares activity.

(e) The high intensity class flares are observed to be rare near the 0°–5° latitude bands. However, the low intensity flares show propensity to occur more near the ±5° latitude band and majorly contributes in the flaring activity.

(f) Using soft X-ray flares data, we found that the southern hemisphere is predominant during solar cycles 21, 22, 23 and 24 in the N–S asymmetry analysis.

(g) In the E–W asymmetry analysis, cycle 21, 22 and 23 are found to be Eastern dominated while cycle 24 is found to be Western dominated.

(h) Our analysis reveals that the N–S asymmetry is highly significant in comparison to E–W asymmetry.

ACKNOWLEDGMENTS

We are thankful to the National Geophysical Data Center (NGDC) and its sister data centers merged into the National Centers for Environmental Information (NCEI), NOAA. We sincerely acknowledge the support extended by Jadavpur University, West Bengal India. This work is a part of RUSA 2.0 Faculty Major Research Project under Jadavpur University (Ref: R-11/437/19).

CONFLICT OF INTEREST

The authors declare that they have no conflicts of interest.

REFERENCES

Badalyan, O.G., Spatial distribution of the N–S asymmetry of solar activity and its time variations, *Astron. Lett.*, 2012, vol. 38, pp. 51–61. https://doi.org/10.1134/S1063773711120024

Badalyan, O.G. and Obridko, V.N., North–south asymmetry of solar activity as a superposition of two realizations: The sign and absolute value, *Astron. Astrophys.*, 2017, vol.603, pp. A109–A119. https://doi.org/10.1051/00046361/201527790

Bai, T., Distribution of flares on the sun during 1955–1985, *Astrophys. J.*, 1987, vol. 314, pp. 795–807. https://doi.org/10.1086/165105

Bai, T., Distribution of flares on the Sun: Superactive regions and active zones of 1980–1985, *Astrophys. J.*, 1988, vol. 328, pp. 860–874. https://doi.org/10.1086/166344

Bankoti, N.S., Joshi, N.C., Pande, B., Pande, S., Uddin, W., and Pandey, K., Asymmetric behavior of different solar activity features over solar cycles 20–23, *New Astron.*, 2011, vol.16, pp. 269–275. https://doi.org/10.1016/j.newast.2010.11.008

Belucz, B., and Dikpati, M., Role of asymmetric meridional circulation in producing north–south asymmetry in a solar cycle dynamo model, *Astrophys. J.*, 2013, vol. 779, p. 4. https://doi.org/10.1088/0004-637X/779/1/4

Carbonell, M., Terradas, J., Oliver, R., and Ballester, J. L., The statistical significance of the North–South asymmetry of solar activity revisited, *Astron. Astrophys.*, 2007, vol. 476, pp. 951–957. https://doi.org/10.1051/0004-6361:20078004

Choudhuri, A.R., The origin of the solar magnetic cycle, *Pramana*, 2011, vol. 77, no. 1, pp. 77–96. https://doi.org/10.1007/s12043-011-0113-4

Chowdhury, P., Choudhary, D.P., and Gosain, S., A study of the hemispheric asymmetry of sunspot area during solar cycles 23 and 24, *Astrophys. J.*, 2013, vol. 768, p. 188. https://doi.org/10.1088/0004-637X/768/2/188

Deng, L.H., Xiang, Y.Y., Qu, Z.N., and An, J.M., Systematic regularity of hemispheric sunspot areas over the past 140 years, *Astron. J.*, 2016, vol. 151, p. 70. https://doi.org/10.3847/0004-6256/151/3/70

Feldman, U., Doschek, G. A., and Klimchuk, J. A., The occurrence rate of soft X-ray flares as a function of solar activity, *Astrophys. J.*, 1997, vol. 474, p. 511. https://doi.org/10.1086/303428

Garcia, H.A., Evidence for solar-cycle evolution of north–south flare asymmetry during cycles 20 and 21, *Sol. Phys.*, 1990, vol. 127, pp. 185–197. https://doi.org/10.1007/BF00158522

Gnevyshev, M.N. and Ohl, A.I., On the 22-year cycle of solar activity, *Astron. Zh.*, 1948, vol. 25, pp. 18–20.

Goel, A., and Choudhuri, A.R., The hemispheric asymmetry of solar activity during the last century and the solar dynamo, *Res. Astron. Astrophys.*, 2009, vol. 9, pp. 115–126.

Heras, A. M., Sanahuja, B., Shea, M. A., and Smart, D. F., Some comments on the east–west solar flare distribution during the 1976–1985 period, *Sol. Phys.*, 1990, vol. 126, pp. 371–383. https://doi.org/10.1007/BF00153057

Javaraiah, J., North–south asymmetry in small and large sunspot group activity and violation of even–odd solar cycle rule, *Astrophys. Space Sci.*, 2016, vol. 361, p. 208. https://doi.org/10.1007/s10509-016-2797-x

Joshi, A., Asymmetries during the maximum phase of solar cycle 22, *Sol. Phys.*, 1995, vol. 157, pp. 315–324. https://doi.org/10.1007/BF00680624

Joshi, B., and Pant, P., Distribution of Hα flares during solar cycle 23, *Astron. Astrophys.*, 2005, vol. 431, pp. 359–363. https://doi.org/10.1051/0004-6361:20041986

Joshi, B., Pant, P., and Manoharan, P.K., North–south distribution of solar flares during cycle 23, *J. Astrophys. Astron.*, 2006, vol. 27, pp. 151–157. https://doi.org/10.1007/BF02702517

Joshi, B., Bhattacharyya, R., Pandey, K.K., Kushwaha, U., and Moon, Y.J., Evolutionary aspects and north–south asymmetry of soft X-ray flare index during solar cycles 21, 22, and 23, *Astron. Astrophys.*, 2015, vol. 581, pp. 1–11. https://doi.org/10.1051/0004-6361/201526369

Joshi, N.C., Bankoti, N.S., Pande, S., Pande, B., and Pandey, K., Study of distribution and asymmetry of solar active prominences during solar cycle 23, *Sol. Phys.*, 2009, vol. 260, pp. 451–463. https://doi.org/10.1007/s11207-009-9446-2

Joshi, N.C., Bankoti, N.S., Pande, S., Pande, B., Uddin, W., and Pandey, K., Statistical analysis of soft X-ray solar flares during solar cycles 21, 22 and 23, *New Astron.*, 2010, vol. 15, pp. 538–546. https://doi.org/10.1016/j.newast.2010.01.002

Komitov, B., and Bonev, B., Amplitude variations of the 11 year cycle and the current solar maximum 23, *Astrophys. J. Lett.*, 2001, vol. 554, p. L119. https://doi.org/10.1086/320908

Kong, D. F., Qu, Z. N., and Guo, Q. L., The north–south asymmetry of solar filaments separately at low and high latitudes in solar cycle 23, *Res. Astron. Astrophys.*, 2015, vol.15, pp. 77–84. https://doi.org/10.1088/1674-4527/15/1/008

Kramynin, A.P., and Mikhalina, F.A., Latitude–longitude characteristics of the north–south asymmetry of solar activity, *Geomagn. Aeron. (Engl. Transl.)*, 2018, vol. 58, pp. 937–941. https://doi.org/10.1134/S0016793218070125

Letfus, V., and Ruzickova-Topolova, B., Time variation of the EW asymmetry of flare numbers with respect to the phase of solar cycles. *Bull. Astron. Inst. Czech.*, 1980, vol. 31, pp. 232–239.

Li, K.J., Schmieder, B., and Li, Q.S., Statistical analysis of the X-ray flares ($M \geq 1$) during the maximum period of solar cycle 22, *Astron. Astrophys. Suppl. Ser.*,1998, vol. 131, pp. 99–104. https://doi.org/10.1051/aas:1998254

Li, K.J., Wang, J.X., Xiong, S.Y., Liang, H.F., Yun, H.S., and Gu, X.M., Regularity of the north–south asymmetry of solar activity, *Astron. Astrophys.*, 2002, vol. 383, pp. 648–652. https://doi.org/10.1051/0004-6361:20011799

Li, K.J., Liu, X.H., Zhan, L.S., Liang, H.F., Zhao, H.J., and Zhong, S.H., Asymmetry of solar active prominences separately at low and high latitudes from 1957 to 1998, *New Astron.*, 2003, vol. 8, pp. 655–664. https://doi.org/10.1016/S1384-1076(03)00053-8

Li, K.J., Gao, P.X., and Zhan, L.S., The long-term behavior of the north–south asymmetry of sunspot activity, *Sol. Phys.*, 2009a, vol. 254, pp. 145–154. https://doi.org/10.1007/s11207-008-9284-7

Li, K.J., Gao, P.X., Zhan, L.S., Shi, X.J., and Zhu, W.W., The north–south asymmetry of solar activity at high latitudes, *Mon. Not. R. Astron. Soc.*, 2009b, vol. 394, pp. 231–238. https://doi.org/10.1111/j.1365-2966.2008.14172.x

Li, K.J., Chen, H.D., Zhan, L.S., Li, Q.X., Gao, P.X., Mu, J., Shi, X.J., and Zhu, W.W., Asymmetry of solar activity in cycle 23, *J. Geophys. Res.: Space Phys.*, 2009c, vol. 114, p. A04101. https://doi.org/10.1029/2009JA014061

Pandey, K.K., Yellaiah, G., and Hiremath, K.M., Latitudinal distribution of soft X-ray flares and disparity in butterfly diagram, *Astrophys. Space Sci.*, 2015, vol. 356, pp. 215–224. https://doi.org/10.1007/s10509-014-2148-8

Parker, E.N., Hydromagnetic dynamo models, *Astrophys. J.*, 1995, vol. 122, p. 293. https://doi.org/10.1086/146087

Schüssler, M. and Cameron, R.H., Origin of the hemispheric asymmetry of solar activity, *Astron. Astrophys.*, 2018, vol. 618, p. A89. https://doi.org/10.1051/0004-6361/201833532

Shetye, J., Tripathi, D., and Dikpati, M., Observations and modeling of north–south asymmetries using a flux transport dynamo, *Astrophys. J.*, 2015, vol. 799, pp. 220–231. https://doi.org/10.1088/0004-637X/799/2/220

Temmer, M., Veronig, A., Hanslmeier, A., Otruba, W., and Messerotti, M., Statistical analysis of solar H flares, *Astron. Astrophys.*, 2001, vol. 375, pp. 1049–1061. https://doi.org/10.1051/0004-6361:20010908

Verma, V.K., On the distribution and asymmetry of solar active prominences, *Sol. Phys.*, 2000, vol. 194, pp. 87–101. https://doi.org/10.1023/A:1005232619582

Viktorinová, B., and Antalová, A., LDE flares in the 21st solar cycle (1976–1986). I. Comparison of the time occurrences of H-alpha and LDE flares, *Bull. Astron. Inst. Czech.*, 1991, vol. 42, pp. 144–157.

Vizoso, G., and Ballester, J. L., The north–south asymmetry of sunspots, *Astron. Astrophys.*, 1990, vol. 229, pp. 540–546. https://doi.org/10.1051/0004-6361:20078004